EXPLORING THE THREE-DIMENSIONAL ARCHITECTURE OF THE CASSINO BASIN FOR LOCAL SEISMIC RESPONSE ANALYSIS

Matteo Albano
Istituto Nazionale di Geofisica e Vulcanologia
matteo.albano@ingv.it

Michele Saroli
Università degli Studi di Cassino e del Lazio meridionale
michele.saroli@unicas.it

Vincenzo Colagiacomo
Università degli Studi di Cassino e del Lazio meridionale
vincenzo.colagiacomo@unicas.it

Matteo Fiorucci
Università degli Studi di Cassino e del Lazio meridionale
matteo.fiorucci@unicas.it

Marco Moro
Istituto Nazionale di Geofisica e Vulcanologia
marco.moro@ingv.it

Fawzi Doumaz
Istituto Nazionale di Geofisica e Vulcanologia
fawzi.doumaz@ingv.it

Abstract

Seismic amplifications depend on the depth of the bedrock, as well as the stratigraphy and dynamic properties of the soil deposits. It is essential to accurately quantify these properties and their uncertainties to assess seismic risk at an urban scale. This paper uses geophysical microtremor measurements, geological and geotechnical surveys, as well as analytical and geostatistical techniques to characterize the complex shape of the bedrock in the Cassino basin, a Quaternary intermontane basin in central Italy. Boreholes, some reaching depths of up to 180 meters, and microtremor measurements are combined to identify the depth of the bedrock by revealing the sharp impedance contrast between the sedimentary/arenaceous bedrock and the soft Quaternary infilling. Understanding the depth of the bedrock is crucial as it influences the propagation of seismic waves to the ground level and is the first step in assessing seismic hazard in the area.

1. Introduction

Central Italy is known for being one of the most seismically active areas in the Mediterranean region. This is evident from the presence of several active faults and the occurrence of strong earthquakes in the past (Rovida *et al.*, 2022). The faults have also played a significant role in shaping the landscapes of the Apennine Mountain chain. The current active extensional tectonics have led to the development of several intermontane basins. These are bordered by active normal faults and are filled with soft

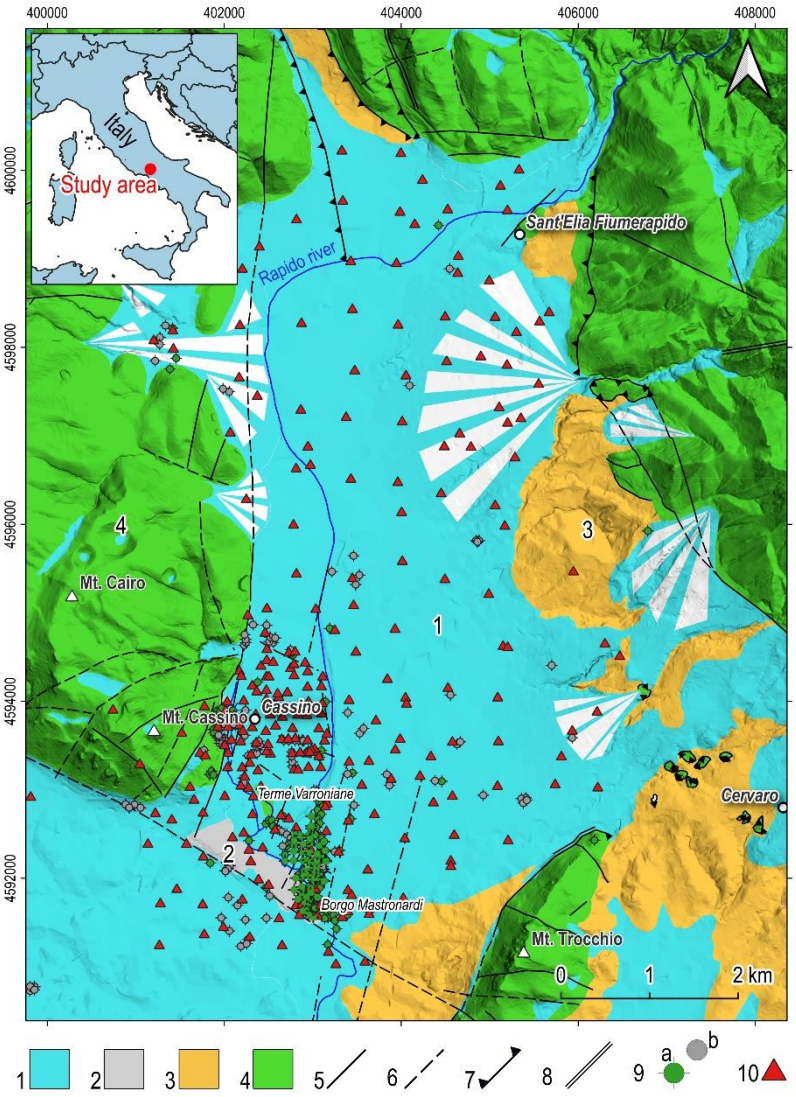

Fig 1. Geological map of the study area, highlighting the main features of the fault system at the surface and the outcropping pre-Quaternary and Quaternary deposits, modified from Saroli et al. (2020). Key to the legend: 1) Recent and old debris, debris fans, eluvial, colluvial and lacustrine soils, interspersed with volcanic products (middle Pleistocene - Holocene). 2) Travertine (Middle Pleistocene - Upper Pleistocene). 3) Sandstones and grey clays (flysch) (Upper Tortonian). 4) Limestones and dolostones with emipelagic marls (Lias - Lower Tortonian). 5) Normal faults. 6) Inferred faults. 7) Thrusts. 8) Strike-slip faults. 9) Boreholes reaching (a) and do not reaching (b) the pre-quaternary sedimentary (n°4) and terrigenous (n°3) basement. 10) Microtremor measurements.

sedimentary soils.

Due to their favourable topographic and environmental conditions, these basins have facilitated the development of ancient settlements in the past and dense urbanization in recent times. The proximity of these settlements to active, seismogenic faults has resulted in high exposure to seismic hazards and risks for many urban settlements, civil infrastructures, industrial centres, and cultural heritage sites. In fact, most of the recent earthquakes in central Italy have caused severe damage and loss of life in intermontane settlements (Locati *et al.*, 2022).

The Cassino basin, located in central Italy, is a remarkable example due to its geological and hydrogeological characteristics. The area is part of a Plio-Pleistocene intermontane basin, situated at the southeastern edge of the Latina Valley. This valley is a broad and narrow depression that formed during the Neogene period along with the Apennines thrust and fold orogenic belt (Fig. 1). The basin has a graben structure that runs northeast to southwest, with the deepest part located in the north. Normal faults dissect the entire area, affecting the transpressive and compressive structures. These segments define the horst-and-graben structure of the basin, with the outcropping limestone platforms of *Terme Varroniane* and *Borgo Mastronardi* representing two intermediate horsts of this system.

Historical and instrumental seismological data indicate that the Cassino basin has experienced powerful earthquakes in the past, with macroseismic intensities as high as grade 9 (Rovida *et al.*, 2022). The probabilistic seismic hazard in this region, calculated from historical earthquakes, is one of the highest in Italy (Meletti and Montaldo, 2007). The peak ground acceleration (PGA) at the bedrock, estimated for a 10% exceedance probability in 50 years, ranges between 0.20 and 0.25 g. These values do not

consider the potential additional amplification caused by soft sedimentary deposits in the area and by critical topographic conditions due to the 3D geometry of the region.
It is important to understand the shape and dynamic features of the soil deposits to accurately analyze seismic hazards. Differences in soil type and rock shape can cause wave reverberation and local ground motion amplification during an earthquake. A first study on the seismic bedrock shape and linear dynamic properties of the soils filling the Cassino basin has been conducted by Saroli et al. (2020). In this study, data from shallow and deep boreholes were collected and interpreted together with microtremor measurements and geophysical surveys to provide a first partial picture of the seismic bedrock morphology and of the linear dynamic properties of the sedimentary infilling.
In this work, we provide a detailed understanding of the shape of the bedrock and the soil's dynamic properties of the whole basin. This will be achieved through a combination of borehole logging, geophysical measurements, and geological-geotechnical surveys to create a 3D model of the basin. This model will then be used in more detailed studies of the area's seismic hazards.

2. Data and methods

A comprehensive study was conducted to analyse the 3D geometry of the subsoil, including quantifying the properties of the overlying layers, identifying impedance contrasts, and determining the depth of the seismic bedrock. We first collected all the available geological and geotechnical data from Saroli et al. (2020), and we integrated this data with new boreholes and microtremor measurements to map the soil resonant frequencies of the whole basin. Finally, we combined the available measurements to estimate the depth of the seismic bedrock.
The collected data consist of stratigraphy from boreholes, geophysical investigations, and laboratory geotechnical investigations. In detail, 132 wells (green circles in Fig. 1) were drilled down to the pre-Quaternary arenaceous and sedimentary bedrock up to 350 m depth for oil research and groundwater exploitation. They allowed us to investigate the morphology of the bedrock and the thickness of Quaternary deposits. The remaining 152 shallow boreholes (grey circles in Fig. 1), drilled in the Quaternary layer only, provide information about the geotechnical properties of the shallow deposits.
A total number of 260 single-station microtremor measurements, performed in three campaigns from 2008 to 2023, were exploited to assess the presence of one or multiple impedance contrasts at depth and to estimate the soil resonant frequency. Measurements were carried out using a three-component LE3D seismometer by Lennartz Electronics GmbH with a 5-second eigenperiod, coupled with a REFTEK 130 datalogger and set to a sampling frequency of 200 Hz. The recording length was approximately 30 to 60 minutes, and it was recommended for spectral analysis to be at least down to 0.5 Hz (Molnar *et al.*, 2022). Microtremor recordings of ambient noise were exploited for the evaluation of the site period (or fundamental frequency) of unconsolidated sediments over high-velocity bedrock according to the noise horizontal-to-vertical spectral ratio method (hereinafter NHVSR) (Nakamura, 1989). The NHVSR curve for each measurement is estimated with the Geopsy code (www.geopsy.org). Parameters adopted to estimate the NHVSR curve are reported by Saroli et al. (2020).
The spatial relationship between the NHVSR-derived resonant frequencies was further enhanced with Kriging interpolation techniques. The latter includes a variety of least-squares methods that provide predictions with the minimum variance of the investigated variable. Such methods can integrate auxiliary information by employing appropriate interpolation algorithms such as co-kriging (CK) and kriging with external drift (KD) (Oliver and Webster, 2014; Trevisani *et al.*, 2017).
First, we performed a preliminary exploratory spatial analysis of the HF to recognize possible correlations, trends, and outliers. Then, we estimated the experimental variogram to identify the presence of possible anisotropies in the data. Finally, we fitted the experimental variogram with a Spherical plus nugget model. The complete analysis was performed using the geostatistical package Gstat (Pebesma, 2004), and experimental data were interpolated with ordinary kriging, together with the associated variance (or standard deviation).

Finally, we estimated the relationship between the depth of the seismic bedrock, i.e., the thickness H of the amplifying layer, at the location where we measured the resonant frequencies by means of the experimental relationship provided in Equation (1):

$$H \cong a \cdot RF^{b} \quad (1)$$

where *RF* is the resonant frequency, *H* is the thickness of the amplifying layer, and *a* and *b* are two coefficients experimentally derived by comparing the resonant frequencies and the bedrock depth at close locations and by best fitting the *RF-H* data with the power-law regression curve of Eq. (1). (D'Amico *et al.*, 2008). Such a relationship provides a simple monotonic relation between *H* and *RF* and implies that the amplifying layer presents a homogenous stiffness.

3. Results

According to Saroli et al. (2020), microtremor measurements performed over the sedimentary and terrigenous lithologies (n.3 and 4 in Fig.1) do not show any significant frequency peaks, thus implying that both lithologies can be classified as seismic bedrock.
NHVSR curves over the quaternary alluvial soils (n.1 in Fig.1) show significant frequency peaks over the range 0.5-15 Hz (Fig.2a), which was associated with the presence of an impedance contrast at depth.

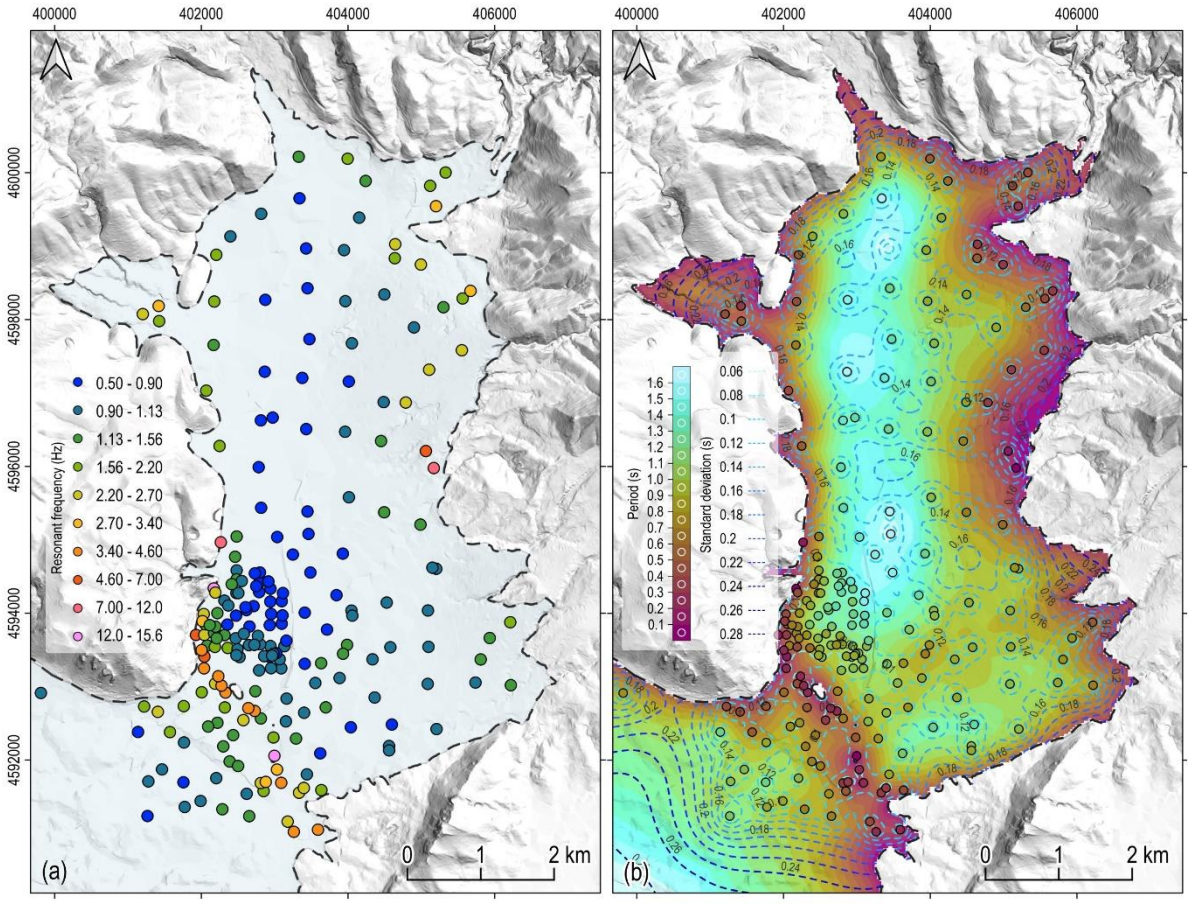

Fig 2. (a) Results of the analysis of microtremor surveys with the NHVSR technique, expressed as peak resonant frequencies, for measurements performed over the quaternary alluvial soils. (b) Results of the geostatistical analysis and Kriging interpolation of soil resonant periods (the coloured circles) over the alluvial plain. The coloured dashed lines identify the standard deviation of the Kriging interpolation.

Moreover, a clear dependency is observed with respect to the distance of the measurements with respect to the outcropping bedrock (hereinafter DOB). For small DOB, peak frequencies are heterogeneous and

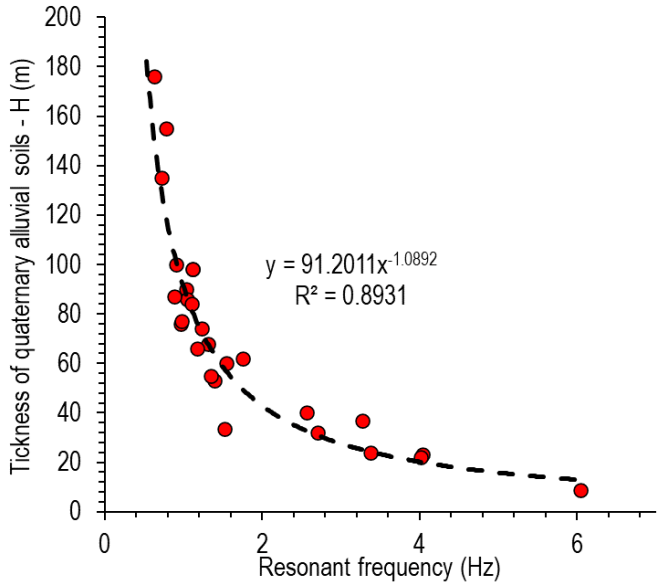

Fig 3. Empirical relationship between resonant frequencies from microtremor measurements and quaternary alluvial soil thickness (H) from nearby deep boreholes.

difficult to interpret because of deviations from the assumption of 1D stratigraphy caused by geometrical and lithological heterogeneities in the subsoil. For higher DOB values, i.e., moving towards the centre of the basin, amplitude peaks shift towards lower frequencies, according to the increase of the bedrock depth (Fig.2a). Indeed, the spatial distribution of the RF values (Fig.2a) shows a strong correlation with the general morphology of the basin. Resonant frequencies in the range of 4–15 Hz result near the Terme Varroniane and Borgo Mastronardi carbonate outcrops and the Mt. Cassino hills, thus testifying to the presence of a shallow impedance contrast. Resonant frequencies gradually decrease, going away from the rocky outcrops to the northwest and southeast, with the lowest values of 0.6-0.8 Hz reaching towards the centre of the Cassino basin.

The spatial mapping of the computed resonant frequencies over the quaternary alluvial soils has been performed employing a geostatistical analysis. To improve the geostatistical interpolation, we worked with resonance periods, as suggested by Trevisani et al. (2017). We also introduced the dependency between the resonant periods and the DOB by using the Kriging with external drift (KD) interpolation technique (Oliver and Webster, 2014), with the DOB assumed as an auxiliary variable in the interpolation procedure. Consequently, the explorative spatial analysis, the estimation of the experimental variogram, and the fitting with a theoretical variogram model have been conducted on data residuals with respect to a trend map that defines the general RP trend in the Cassino basin. The experimental variogram has been analysed using both variogram cloud, variogram map, and directional and omnidirectional variograms, showing the absence of anisotropies, local outliers, or other patterns related to non-stationarity. The final isotropic experimental variogram has been fitted with the isotropic spherical plus nugget model. Once the theoretical variogram of the resonant period residuals was defined, we interpolated the resonant periods together with the trend map using KD. Details about the exploratory spatial analysis, the variogram analysis, the geostatistical interpolation, and the cross-validation analysis of the KD interpolation are reported in Saroli et al. (2020).

Fig. 2b shows the obtained resonant period map, while the predicted resonant period map's standard deviation error is represented in the same figure with dashed curves coloured with shades of blue according to the standard deviation values. The shape of the obtained maps agrees with the tectonic evolution of the basin, characterized by a horst-and-graben structure where boundary faults acted as the main dislocating features. Resonant periods range from 0.1 s close to the bedrock boundary and to the outcrops of *Borgo Mastronardi* and *Terme Varroniane*, to values up to 1.7 s towards the center of the basin, along an approximately N-S oriented depocenter.

These values mimic the presence of soil deposits of variable thickness filling the basin. In particular, a correlation between the experimental resonant periods from microtremor measurements and the nearby deep boreholes in the plain has been defined according to Equation 1. This relation (Fig.3) allowed us to convert resonant frequency values in equivalent virtual boreholes to identify the depth of the seismic bedrock corresponding to the sedimentary and terrigenous outcrops (n.3 and 4 in Fig.1).

4. Conclusions and further developments

The analysis of multiple microtremor measurements conducted in the Cassino Basin has allowed us to identify a contrast in impedance at depth, specifically at the transition from quaternary alluvial deposits to carbonatic and arenaceous bedrock. The extensive number of measurements has also enabled us to create a map showing the resonant period of the alluvial deposits in the basin, revealing the complex horst-and-graben system characterizing the area. Through joint analysis with available deep boreholes, we have been able to estimate the experimental relationship between soil resonant frequency and thickness. This has provided us with several virtual boreholes, which can be used alongside existing boreholes to define the complex morphology of the seismic bedrock. Our future efforts will focus on reconstructing the geometry of the bedrock, considering the presence of major and minor fault segments dislocating the plain. Geotechnical data from in situ and laboratory surveys will also be utilized to assess the geotechnical and dynamic properties of the quaternary alluvial soils, in addition to evaluating their liquefaction potential. These analyses will form the basis for developing dynamic numerical models of the area, allowing us to assess local site amplification and the interaction with existing buildings and infrastructures.

Bibliography

D'Amico V. *et al.* (2008). "Ambient Noise Measurements for Preliminary Site-Effects Characterization in the Urban Area of Florence, Italy", *Bulletin of the Seismological Society of America*, 98(3), pp. 1373–1388. https://doi.org/10.1785/0120070231.

Locati M. *et al.* (2022). "Database Macrosismico Italiano (DBMI15), versione 4.0". Istituto Nazionale di Geofisica e Vulcanologia (INGV). Available at: https://doi.org/10.13127/DBMI/DBMI15.4.

Meletti C. and Montaldo, V. (2007). *Stime di pericolosità sismica per diverse probabilità di superamento in 50 anni: valori di ag.* Deliverable D2.

Molnar S. *et al.* (2022). "A review of the microtremor horizontal-to-vertical spectral ratio (MHVSR) method", *Journal of Seismology*. https://doi.org/10.1007/s10950-021-10062-9.

Nakamura Y. (1989). "A method for dynamic characteristics estimation of subsurface using microtremor on the ground surface.", *Quarterly Report of Railway Technical Research*, 30, pp. 25–33.

Oliver M.A. and Webster, R. (2014). "A tutorial guide to geostatistics: Computing and modelling variograms and kriging", *CATENA*, 113, pp. 56–69. https://doi.org/10.1016/j.catena.2013.09.006.

Pebesma E.J. (2004). "Multivariable geostatistics in S: the gstat package", *Computers & Geosciences*, 30(7), pp. 683–691. https://doi.org/10.1016/j.cageo.2004.03.012.

Rovida A. *et al.* (2022). "Catalogo Parametrico dei Terremoti Italiani (CPTI15), versione 4.0". Istituto Nazionale di Geofisica e Vulcanologia (INGV). https://doi.org/10.13127/CPTI/CPTI15.4.

Saroli M. *et al.* (2020). "Insights into bedrock paleomorphology and linear dynamic soil properties of the Cassino intermontane basin (Central Italy)", *Engineering Geology*, 264, p. 105333. https://doi.org/10.1016/j.enggeo.2019.105333.

Trevisani S. *et al.* (2017). "Insights into bedrock surface morphology using low-cost passive seismic surveys and integrated geostatistical analysis", *Science of The Total Environment*, 578, pp. 186–202. https://doi.org/10.1016/j.scitotenv.2016.11.041.